Surface Investigations Using the Positron Reemission Microscope

James Van House and Arthur Rich
Department of Physics, The University of Michigan, Ann Arbor, Michigan 48109
(Received 6 May 1988)

We have constructed a positron reemission microscope and taken images of a number of targets using it. The unique image contrast of this device is determined by the probability that positrons are remitted from a specimen surface. The surface and near-surface defect sensitivity of the positron reemission microscope is demonstrated, as well as the feasibility of imaging biological specimens and semiconductor devices. Applications are discussed.

PACS numbers: 07.80.+x, 41.80.−y

In this article we present detailed results obtained with a positron reemission microscope (PRM).[1] The PRM is based on the phenomenon of spontaneous reemission of low-energy ($\simeq 1$ eV) positrons (e^+) from the surface of a sample, after implantation of an initially higher-energy (1-10 keV) e^+ beam within roughly a diffusion length of the sample surface. Up to 50% of the incident e^+ can be reemitted as slow e^+, which are then accelerated and focused to form an image of the reemitting surface. The image contrast is determined by any process that affects the probability of an e^+ diffusing to and being reemitted from the sample surface. Such processes include bulk, interface and surface defect trappings, positronium (Ps) formation, and the effects of adsorbates and thin-film overlayers. We have used our PRM to obtain imaging information from a variety of surfaces, including biological specimens and semiconductor devices, and we have also successfully obtained images which utilize the unique sensitivity of e^+ to defect trapping.

The PRM, as well as the transmission positron microscope[2] (TPM) and the e^+ microprobe,[3] belong to a class of e^+ imaging devices which exploit the different contrasts offered by e^+ vs e^-. The PRM differs from these other e^+ imaging devices in that the nature of the low-energy e^+ emission process and the short depth of field of the imaging optics combine to make it an extremely surface-sensitive device, sampling e^+ interactions which occur at an energy of 0-3 eV. By comparison, in the TPM, contrast formation occurs for e^+ interactions at energies of 2 keV and above, thereby causing the TPM to sample primarily bulk properties of thin targets. The areas of application of the PRM are thus radically different from those of the TPM. While surface sensitivity will also be present in the scanning e^+ microprobe,[3] its resolution will be limited by the combined variation (typically 100-1000 Å) in the e^+ implantation depth plus any e^+ diffusion prior to emission of the e^+ signal. As discussed below, the resolution of the surface and near-surface information available in the PRM images should ultimately be better.

Although the PRM is clearly distinct from standard electron microscopes, it is useful to compare it with two electron-microscope analogs: the electron field emission microscope and the photoelectron emission microscope. A PRM based on a transmission geometry, where a small sample is placed on a thin ($\simeq 1000$ Å) e^+ emitting substrate,[4] was first suggested in 1984[5] and compared with a field emission microscope. The analysis[5] suggested that it might be possible to achieve higher resolutions in the imaging of the edges of the sample shadow when the PRM is used, because of the smaller transverse energy spread[6] (high emittance) of reemitted e^+. Furthermore, because e^+ are emitted spontaneously, significantly smaller accelerating fields are required for imaging, resulting in reduced sample damage. If, however, instead of shadowing a sample edge, the sample itself serves as the e^+ emitting surface, the image contrast will incorporate new physics from a variety of e^+ specific interactions within the sample. Such *direct* imaging of e^+ reemission from a sample is analogous to the photoelectron emission microscope.[7]

The instrument we have built is shown in Fig. 1 and described in detail in the caption. It is designed in a reflection (rather than transmission) geometry[8] which allows direct imaging of thick targets. The reflection geometry offers great flexibility in the choice and preparation of targets, making it particularly useful for applications in, for example, surface physics and materials sciences. The geometry also allows the implantation of the incident e^+ into the sample at a depth controlled by the incident beam energy, resulting in the ability to depth profile subsurface features. The major drawback is a 2-3 times lower ultimate resolution, as discussed below.

The resolution of the features which will appear in the direct images will be determined by a convolution of physical effects, such as e^+ diffusion, and the instrumental aberrations of the imaging optics. The resolution of features containing information determined by *bulk* e^+ interactions will be limited by the e^+ thermal diffusion length (typically 100-1000 Å). On the other hand, variations in the reemission rate due to surface states or defects, thin-film overlayers, adsorbates, etc., will occur near the point of e^+ emission, resulting in potentially

© 1988 The American Physical Society

higher resolution for surface and near-surface phenomena. Depending on the details of the e^+ reemission process, the resolution can be as small as a few angstroms for reemission phenomena such as e^+ interactions with thin-film overlayers, rendering the PRM an extremely surface-sensitive instrument. The resolution of the PRM for such phenomena will then be determined by the instrumental resolution.

The instrumental resolution, R, which is the spatial resolution in object space of the electron optical system, depends on the parameters of the incident slow e^+ beam and the target, as well as on the aberrations of the electron optical system. The value of R can be readily obtained from Eq. (3) of Ref. 2, which applies to the TPM, if this equation is modified to reflect the fact that, whereas in the TPM the resolution was determined by the properties of the moderator (or remoderator) used to generate the slow e^+ beam, in the PRM the *target* serves as the moderator for those e^+ which are subsequently used to form an image. Consequently, all quantities which relate to the moderator in Eq.(3) of Ref. 2 must now be replaced with the corresponding target properties. The result of this straightforward replacement is that Eq. (3) of Ref. 2 may be rewritten[9] as

$$R=\left\{\frac{C_c}{3}\left(\frac{\Delta V_e}{V_a}\right)\left(\frac{V_e}{V_a}\right)^{1/2}\sin\theta_e\left(\frac{\rho_d}{P(E)\rho_t}\right)^{1/2} r_d\left[1+\left(1+\frac{9C_s r_d\sin\theta_e[\rho_d V_e/P(E)\rho_t V_a]^{1/2}}{(C_c\Delta V_e/V_a)^2}\right)^{1/2}\right]\right\}^{1/2}. \quad (1)$$

Here, V_a is the accelerating potential of the anode (all potentials are taken with respect to the target potential), V_e is the reemitted e^+ emission energy, expressed in volts, ΔV_e is the variation in V_e,[7] θ_e is the angle of e^+ emission with respect to the target normal, r_d is the width of the single-particle spot produced by the channel electron multiplier array (in Fig. 1) and ρ_d is the e^+ current density at the detector. The quantity ρ_t is the current density of the *incident* beam at the target, prior to its thermalization within the target, while $P(E)$ is the energy (E) dependent e^+ reemission probability, averaged over the PRM field of view. The quantities C_s and C_c are the spherical and chromatic aberration coefficients of the electron optical system. These coefficients consist of an appropriately weighted combination of the aberrations of the projector lens (which are negligible), and the objective lens, as well as the aberrations due to the electric field used to accelerate the reemitted e^+ from the target to the anode.[7] The aberrations due to this electric field (not present in the TPM) are larger than those of the objective lens for fields of 10 kV/cm and above,[7] but can be ignored for the conditions which obtain in our instrument.[8] The strongest dependence of R on target properties appears in Eq. (1) through $P(E)$, since it can vary by more than 10^3 from one target to another. A detailed discussion of the dependence of R on the other parameters in Eq. (1) can be found in Ref. 2.

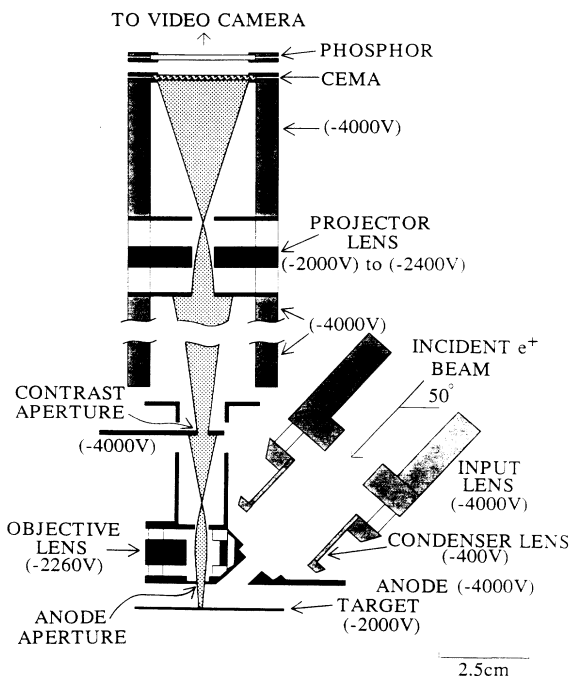

FIG. 1. The positron reemission microscope. The incident beam of 5×10^5 e^+/s, discussed in detail in Ref. 2, is generated by a 40-mCi ^{22}Na-source, W-vane-moderator combination. This beam is directed into the input lens and is then focused by the condenser lens onto a 2.5-mm-diam spot at the target, at an incident energy of 2 keV. The reemitted e^+ are accelerated by the electric field between the target and anode, focused by the lensing effect of the anode aperture and then by the objective lens to the projector lens. The projector lens images the e^+ onto a channel electron multiplier array (CEMA) with a phosphor screen anode which generates a 100-μm-diam spot of light for each incident e^+. This spot is detected by a video camera and signal averaged by an image analysis system as described in Ref. 2. The signal averaging is necessary, because of the low e^+ flux (10^{-18}–10^{-17} A/cm^2) at the CEMA detector.

The parameters which characterize our PRM are $C_s=50$ cm, $C_c=20$ cm, $\rho_t=2\times10^{-12}$ A/cm^2, $r_d=1\times10^{-2}$ cm, $\rho_d=2\times10^{-17}$ A/cm^2, and $V_a=E=2$ kV. Thus, for the target parameters $P(E)=0.2$ and $V_e=\Delta V_e=2$ V, typical of many metal samples,[10] Eq. (1) yields $R=4$ μm. In the actual operation of the microscope, however, a highly restrictive contrast aperture was found to be necessary to suppress a background caused by e^+ which elastically scattered from the target. These elastically scattered e^+ would otherwise form a central "bright spot" in images where low values of $P(E)$ resulted in a low signal-to-noise ratio. The restrictive contrast aperture improved R to 0.15 μm, at the cost of longer signal averaging times. The image resolution, therefore, was determined entirely by the detector resolution, $R_d=r_d/M$, where M is the magnification which, in our instrument, varied between 15× and 55×.

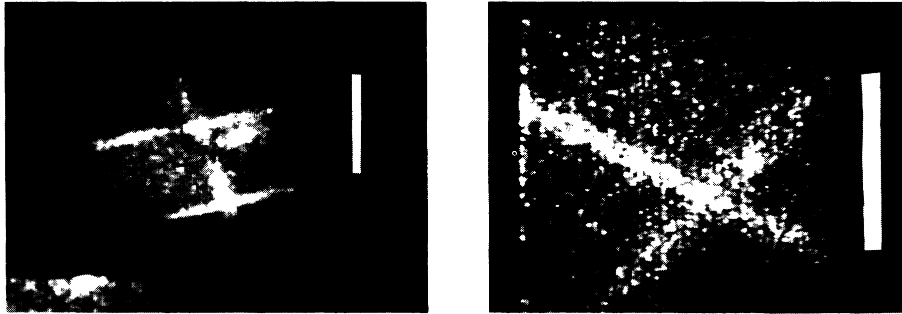

FIG. 2. A demonstration of the near-surface defect sensitivity of the PRM. The preparation of the damaged W and Mo foils is described in the text. The dark sputtered regions have low e^+ reemission due to e^+ trapping in defects. The bright high reemission areas were masked from sputter damage. The image on the left is the argon-sputtered W foil and was taken at $M = 28\times$ ($R = 4.6$ μm) and required 8 h to accumulate. The white bar on the right-hand side represents 250 μm. The image on the right is the N_2 bombarded Mo foil and was taken at $M = 56\times$ ($R = 2.3$ μm). It required 30 h to accumulate. The white bar represents 125 μm.

Images were taken of a variety of targets which either demonstrate a unique e^+ contrast or the feasibility of direct imaging of samples which are of potential interest. All images were obtained after adjustment of the objective lens voltage until selected image features were in focus. Magnifications were determined from calibration foils with features of known size. Resolutions were measured through use of a Gaussian fit to an intensity profile of a sharp edge within the image.

In order to exploit the known[11] sensitivity of e^+ reemission to the density of surface and near-surface defects, images were obtained of ion-bombarded W and Mo foils. Prior to ion bombardment, the W and Mo foils were prepared by a 4-h annealing at 2200 and 1400 °C, respectively, in a diffusion-pump vacuum of 10^{-5} Torr, resulting in reproducible values of $P(E) \sim (15\text{–}20)\%$ in the PRM vacuum of 10^{-6} Torr. Heating of the foils to 900 °C in the PRM for extended periods did not appreciably change $P(E)$. Auger-electron spectroscopy indicates that the surfaces consisted of oxides of W or Mo, with some carbon contamination.

The images obtained are shown in Fig. 2. For one image, a W foil target was masked with a 100 line, 82% transmitting Cu grid and sputtered at normal incidence with 2-keV argon ions to a fluence of $\simeq 10^{16}/\text{cm}^2$. The Mo target was similarly masked, and then bombarded with 40-keV N_2 ions to a fluence of $2.5\times 10^{15}/\text{cm}^2$. The resulting images, after removal of the masks, unambiguously demonstrate defect maps of the surfaces. This defect sensitivity will be of particular interest in the study of surface atom diffusion and surface diffusion of defects in a variety of materials, including semiconductors. We did in fact image two semiconductor devices, for which $P(E)$ was determined, from the measured transmission of the electron optical system and the measured detector rate, to be 1%. This rate was found to be sufficient to demonstrate contrast between circuitry and the somewhat darker silicon substrate, but was not sufficient to allow magnifications high enough to resolve individual circuit elements in a reasonable signal averaging time. The defect sensitivity of the PRM may also be useful in studies of the role of surface defects in crack formation.

We have also demonstrated the feasibility of imaging biological specimens (Fig. 3). The image in Fig. 3 also demonstrates materials contrast, in this case, between the specimen and the dark, low-reemission, silver-foil substrate. Typical emission rates from such samples were $P(E) \sim (2\text{–}4)\%$, suggesting that 5–10 times longer running times, or higher values of ρ_t, are necessary to obtain resolutions for biological specimens comparable to that of metals.

Modifications to our PRM now underway will include (i) straightforward improvements in the beam optics and

FIG. 3. This image demonstrates the feasibility of direct imaging of biological specimens with the PRM, and also demonstrates materials constrast. A single strand of hair was placed on a silver-foil conducting substrate (dark background). This substrate was chosen for its low e^+ reemission [$P(E) \simeq 0.3\%$], highlighting the high specimen reemission [$P(E) \sim 2\%$]. The magnification is $M = 15\times$ and $R = 15$ μm. The image required 20 h of signal averaging to accumulate. The white bar represents 100 μm. Sample charging may have contributed to degraded image quality and resolution.

in the image detection and data analysis system which will allow a factor of 10 decrease in overall image resolution (to of order 0.2 μm); (ii) implementation in an ultrahigh vacuum system, which would allow the characterization of the sample surface. In addition, we plan to consider the feasibility of incorporating an energy analyzer with an energy resolution of about 0.1 eV so that high spatial resolution imaging could be combined with reemitted e^+ spectroscopy[12] of thin metal films and multilayer systems. One could then selectively image layers of a specific material, as well as image alloyed or pseudomorphically deformed layers,[12] and possibly even overlayer islands for studies of nucleation and growth. Further improvements in the PRM resolution by 10^2 or more are feasible by increasing ρ_t, along with appropriate redesign of the electron optical system. We calculate that, for our reflection geometry,[8] and $V_a = 5$ kV, R will approach the diffraction limit on resolution[2] of 20 Å at $\rho_t = 1\times10^{-7}$ A/cm^2. Values of $\rho_t \simeq 10^{-9}$ A/cm^2 have already been achieved with the brightness-enhanced[13] slow e^+ beam used in the e^+ microprobe.[3] Noting[2] that R is approximately proportional to $\rho_t^{-3/8}$, we calculate that at this value of ρ_t, R less than 100 Å is possible. Values of $\rho_t \simeq 10^{-7}$ A/cm^2 can be achieved by combination of brightness enhancement with the use of higher activity radioactive sources,[14] or LINAC based e^+ beams,[15] as well as by use of improved moderators.[16]

In conclusion, we have taken images using a positron reemission microscope and discussed some of its areas of application. The defect sensitivity of the PRM contrast, as well as the feasibility of imaging semiconductors and biological specimens is demonstrated. The information obtained from such images is necessary for future planned improvements of the PRM and for the program of studies using positron reemission microscopy now underway in our laboratory.

We wish to acknowledge R. Conti, W. E. Frieze, M. Mauck, G. Rempfer, M. Skalsey, and P. W. Zitzewitz for useful discussions. We particularly acknowledge D. W. Gidley for critical discussions of this work and D. W. Gidley and the Michigan Ion Beam Laboratory for technical assistance. This research was supported by the National Science Foundation (Grant No. PHY-8403817) and the University of Michigan under a grant from the Office of the Vice President for Research.

---

[1]An announcement of the PRM was published in J. Electron Microsc. Tech. **9**, 209 (1988).

[2]J. Van House and A. Rich, Phys. Rev. Lett. **60**, 169 (1988).

[3]G. R. Brandes, K. F. Canter, T. N. Horsky, P. H. Lippel, and A. P. Mills, Jr., Rev. Sci. Instrum. **59**, 228 (1988), and Bull. Am. Phys. Soc. **32**, 439 (1987).

[4]P. J. Schultz, E. M. Gullikson, and A. P. Mills, Jr., Phys. Rev. B **34**, 442 (1986).

[5]L. D. Hulett, J. M. Dale, and S. Pendyala, Mater. Sci. Forum **2**, 133 (1984).

[6]C. A. Murray and A. P. Mills, Jr., Solid State Commun. **34**, 789 (1980); E. M. Gullikson *et al.*, Phys. Rev. B **32**, 5484 (1985).

[7]O. H. Griffen and G. F. Rempfer, in *Advances in Optical and Electron Microscopy,* edited by R. Barer and V. E. Cosslett (Academic, New York, 1986), Vol 10, and references therein.

[8]A full discussion of the instrumental details will be submitted for publication shortly.

[9]Equation (1) in Ref. 2 does not conform to standard electron microscopy notation. This is rectified here by the substitions $C_s/4 \longrightarrow C_s$ and $C_c \longrightarrow 2C_c$. This does not change the numerical results in Ref. 2, which took the nonstandard notation into account.

[10]J. Van House and P. W. Zitzewitz, Phys. Rev. A **29**, 96 (1984).

[11]P. J. Schultz, K. G. Lynn, W. E. Frieze, and A. Vehanen, Phys. Rev. B **27**, 6626 (1983); A. R. Koymen, D. W. Gidley, and T. W. Capehart, Phys. Rev. B **35**, 1034 (1987), and references therein.

[12]D. W. Gidley and W. E. Frieze, Phys. Rev. Lett. **60**, 1193 (1988).

[13]A. P. Mills, Jr., Appl. Phys. **23**, 189 (1980); W. E. Frieze, D. W. Gidley, and K. G. Lynn, Phys. Rev. B **31**, 5628 (1985).

[14]D. M. Chen *et al.*, Phys. Rev. Lett. **58**, 921 (1987); E. H. Ottewitte, in *Advanced Accelerator Concepts—1986,* edited by F. E. Mills, AIP Conference Proceedings No. 156 (American Institute of Physics, New York, 1987).

[15]I. J. Rosenberg, R. H. Howell, and M. J. Fluss, Phys. Rev. B **35**, 2083 (1987).

[16]E. Gullikson and A. P. Mills, Jr., Phys. Rev. Lett. **57**, 376 (1986).

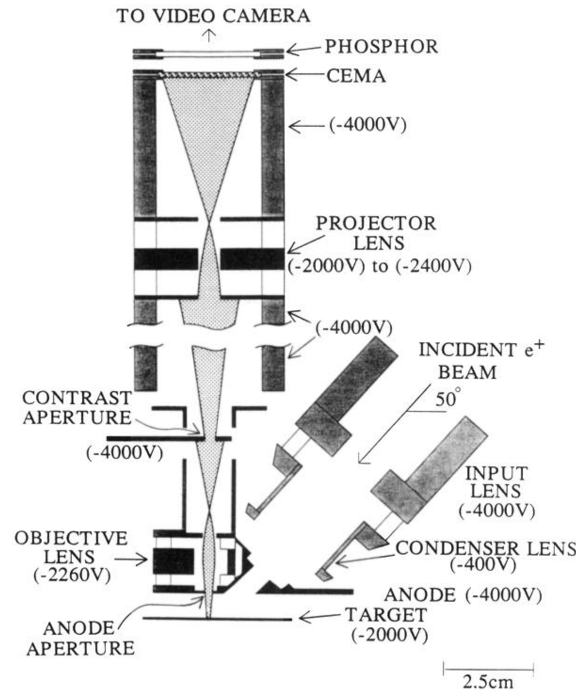

FIG. 1. The positron reemission microscope. The incident beam of 5×10^5 e^+/s, discussed in detail in Ref. 2, is generated by a 40-mCi ^{22}Na-source, W-vane-moderator combination. This beam is directed into the input lens and is then focused by the condenser lens onto a 2.5-mm-diam spot at the target, at an incident energy of 2 keV. The reemitted e^+ are accelerated by the electric field between the target and anode, focused by the lensing effect of the anode aperture and then by the objective lens to the projector lens. The projector lens images the e^+ onto a channel electron multiplier array (CEMA) with a phosphor screen anode which generates a 100-μm-diam spot of light for each incident e^+. This spot is detected by a video camera and signal averaged by an image analysis system as described in Ref. 2. The signal averaging is necessary, because of the low e^+ flux (10^{-18}–10^{-17} A/cm^2) at the CEMA detector.

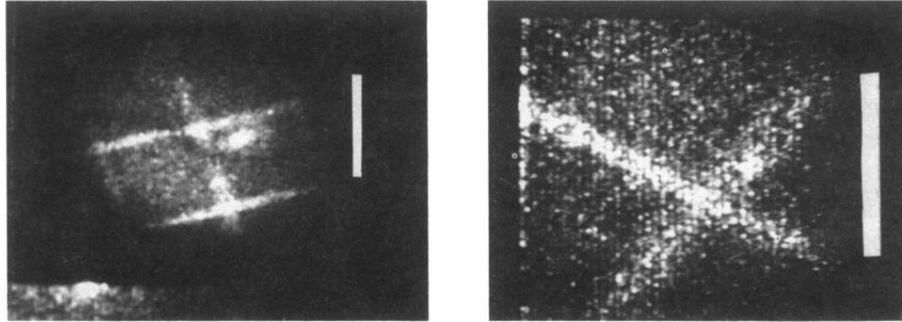

FIG. 2. A demonstration of the near-surface defect sensitivity of the PRM. The preparation of the damaged W and Mo foils is described in the text. The dark sputtered regions have low e^+ reemission due to e^+ trapping in defects. The bright high reemission areas were masked from sputter damage. The image on the left is the argon-sputtered W foil and was taken at $M = 28\times$ ($R = 4.6$ μm) and required 8 h to accumulate. The white bar on the right-hand side represents 250 μm. The image on the right is the N_2 bombarded Mo foil and was taken at $M = 56\times$ ($R = 2.3$ μm). It required 30 h to accumulate. The white bar represents 125 μm.

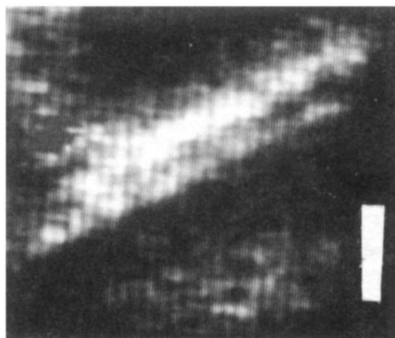

FIG. 3. This image demonstrates the feasibility of direct imaging of biological specimens with the PRM, and also demonstrates materials constrast. A single strand of hair was placed on a silver-foil conducting substrate (dark background). This substrate was chosen for its low e^+ reemission [$P(E) \simeq 0.3\%$], highlighting the high specimen reemission [$P(E) \sim 2\%$]. The magnification is $M = 15\times$ and $R = 15$ μm. The image required 20 h of signal averaging to accumulate. The white bar represents 100 μm. Sample charging may have contributed to degraded image quality and resolution.